Journal of Alloys and Compounds 583 (2014) 309–312

Contents lists available at ScienceDirect

Journal of Alloys and Compounds

journal homepage: www.elsevier.com/locate/jalcom

Hydrothermal synthesis of $DyMn_2O_5$ nanorods and their magnetic properties

Songping Wu *, Youxian Mei

School of Chemistry and Chemical Engineering, South China University of Technology, Guangzhou 510641, China

ARTICLE INFO

Article history:
Received 24 June 2013
Received in revised form 18 August 2013
Accepted 19 August 2013
Available online 8 September 2013

Keywords:
Multiferroics
Nanomaterials
Magnetically ordered materials
Crystal growth
Magnetic measurements

ABSTRACT

Highly pure $DyMn_2O_5$ nanorods have been synthesized via hydrothermal route. FT-IR and Raman patterns were employed to determine $DyMn_2O_5$. PLE and PL spectra of $DyMn_2O_5$ showed UV excitation and near band edge (NBE) emission. Magnetic measurement indicated the crystalline $DyMn_2O_5$ showed a weak ferromagnetic ordering due to incomplete spin compensation on the surface. The ferromagnetic transition could be explained by an antiferromagnetic core and a ferromagnetic surface.

1. Introduction

The orthorhombic RMn_2O_5 (R = rare earth, Bi, Y) are currently of great interest. Members of the family RMn_2O_5 are unique because they undergo an antiferromagnetic (AFM) transition at Néel temperature T_N = 39–45 K, whereas a ferroelectric transition occurs at (or slightly below) T_N for the Mn spin sublattice. In high temperature, the RMn_2O_5 magnetic structure is almost paramagnetic [1,2].

$DyMn_2O_5$ belongs to the orthorhombic family RMn_2O_5, in which the Mn atoms are present in the ionic states Mn^{3+} and Mn^{4+} and occupy two different crystallographic sites [1]. $DyMn_2O_5$ displays the strongest ferroelectric polarization and magnetodielectric effect of the RMn_2O_5. In $DyMn_2O_5$, both the Dy and Mn moments lie close to the "b" axis, whereas in other RMn_2O_5 they lie close to the "*a*" axis [3]. Strong lattice anomalies as a function of the magnetic field are detected at the low temperature magnetic and ferroelectric phase transitions [4]. The unusual combination of magnetic frustration and strong magnetoelastic coupling is responsible for the remarkable changes of the dielectric properties of colossal magnetoelectric $DyMn_2O_5$ in small applied magnetic fields [5].

The conventional solid-state method is often used to prepare multiferroic material $DyMn_2O_5$ [3–5]. Koo grew highly epitaxial $DyMn_2O_5$ thin films on Nb-doped TiO_2 (110) single crystal substrates by using the pulsed laser deposition technique [6]. Recently, hydrothermal synthesis has attracted more interest for its advantages of process simplicity (one-step) and low-temperature. In previous works, some multiferroics materials have been selectively synthesized through the hydrothermal route, such as $BiFeO_3$ nanowires [7], $TbMn_2O_5$ nanorods [8], $BiMn_2O_5$ crystals [9], $BaMnO_3$ nanoparticles [10], RMn_2O_5 (R = Gd and Sm) nanorods and nanoplates [11], RMn_2O_5 (R = La, Pr, Nd, Tb, Bi) and $LaMn_2O_{5+d}$ [12], RMn_2O_5 (R = Gd, Sm Yb) [13] and YMn_2O_5 nanorods [14].

In this paper, the $DyMn_2O_5$ nano-crystallites were synthesized by hydrothermal route. We also investigated the photoluminescence (PL) and magnetic properties of $DyMn_2O_5$ nanorods.

2. Experimental

The raw materials included $Dy(NO_3)_3{\cdot}6H_2O$, $KMnO_4$ and $MnCl_2{\cdot}4H_2O$. All chemicals were analytical grade and used without further purification. In a typical experiment, firstly, 2 mmol $Dy(NO_3)_3{\cdot}6H_2O$ was dissolved in a 100 ml beaker with 60 ml distilled water and then 2.8 mmol $MnCl_2{\cdot}4H_2O$ and 1.2 mmol $KMnO_4$ were dissolved in the solution under constant magnetic stirring. The molar ratio of Mn^{2+}: Mn^{7+} was 7:3. Secondly, after the solution was stirred using a magnetic bar for 30 min at room temperature, the NaOH solution was added to the above uniform solution to adjust the pH value. Finally, the mixtures were transferred into a Teflon-lined stainless steel autoclave with an inner volume 80 ml. The autoclaves were sealed and placed in a digital-type temperature-controlled oven at the appropriate temperatures for 64 h. After reaction completion, the solution was cooled down to room temperature naturally. The obtained products were filtered out and washed with distilled water for several times. The final powders were dried at 60 °C overnight.

The crystalline phases of the specimens were analyzed by X-ray diffraction (XRD) (D8 Advance, Bruker, Germany) with Cu Kα radiation of 2θ from 10 to 70°. The unit cell parameters were refined using Jade 6.0 software. The transmission electron microscope (TEM), high-resolution transmission electron microscope

* Corresponding author. Tel.: +86 20 87112897.
E-mail address: chwsp@scut.edu.cn (S. Wu).

0925-8388/$ - see front matter © 2013 Elsevier B.V. All rights reserved.
http://dx.doi.org/10.1016/j.jallcom.2013.08.131

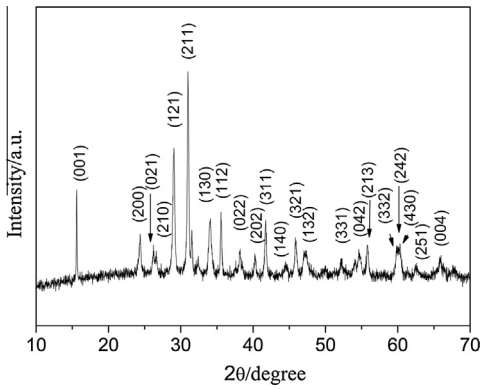

Fig. 1. XRD pattern of $DyMn_2O_5$ nanorods synthesized at 250 °C (pH = 3).

(HRTEM) and selective area electron diffraction (SAED) images were taken with a JEM-2100HR electron microscope (JEOL, Tokyo, Japan) with an accelerating voltage of 200 kV. Element analysis of microdomain was carried out with an energy dispersive spectrometer (EDS) (EPMA1600, Shimadzu, Japan). FT-IR spectra were obtained using a Fourier transform infrared spectrometer (Vector 33, Brucker, Germany). Raman spectra of $DyMn_2O_5$ nanorods were obtained with Micro-raman spectrometer (LabRAM Aramis, HJY, France). The photoluminescence (PL) and photoluminescence excitation (PLE) spectra were measured using a fluorescence spectrometer (F-4500, Hitachi, Japan). The magnetic characteristic was measured by a physical property measurement system (PPMS) from Qyantum Design Inc. USA.

3. Results and discussion

Fig. 1 shows a typical XRD pattern of $DyMn_2O_5$ synthesized at 250 °C for 64 h (pH = 3). All the peaks could be readily indexed to a pure orthorhombic $DyMn_2O_5$. The calculated lattice parameters of $DyMn_2O_5$ were $a = 0.7295$ nm, $b = 0.8502$ nm and $c = 0.5679$ nm, which are consistent with the standard values (JCPDS No. 72–1696). No peaks of other impurity phases can be observed, indicating that highly pure $DyMn_2O_5$ nano-crystalline were obtained.

Monodispersed $DyMn_2O_5$ nanorods were characterized by TEM in Fig. 2. Those nanorods are with 400–600 nm in length and 100 nm in diameter as pH = 3 (Fig. 2a); however, aspect ratio becomes small as pH increased to 7 (Fig. 2(f)). The image also shows that the nanorods with smooth surface are terminated by semi-circular closed tips. The HRTEM image at the edge of the $DyMn_2O_5$ nanorods (Fig. 2(b) and (c)) displays a good single crystalline structure. The spacing of 0.263 nm corresponds to that of (1 3 0) lattice plane of the $DyMn_2O_5$. The corresponding SAED pattern (Fig. 3(d)) showed the single-crystalline nature of the $DyMn_2O_5$ nanorods. EDS showed that the molar ratio of Dy: Mn was 1:2 (Fig. 2(e)).

FT-IR spectrum of the $DyMn_2O_4$ nanorods was shown in Fig. 3(a). In the spectrum, absorption peaks at 442 cm^{-1} and 535 cm^{-1} could be ascribed to asymmetric stretching vibration of DyO_6 octahedron [15,16]. Absorption peak at 640 cm^{-1} corresponded to Mn–O bending vibration [17].

The local atomic structure of $DyMn_2O_4$ nanorods was characterized by Raman spectroscopy (see Fig. 3(b)). Those peaks at 218, 350, 465, 502, 634, and 706 cm^{-1} were assigned to A_g mode of orthorhombic $DyMn_2O_5$. Those peaks located at 634 and 706 cm^{-1} were attributed to stretching vibration modes of Mn–O [2]. The lines at ~300 cm^{-1} corresponded to modes involving mainly stretching and bending vibrations of light oxygen atoms, whereas those at lower frequencies involve motions of heavier Mn and Ho (Tb) atoms. Most of the lines in the low-frequency range are extremely sharp, indicating weak an harmonicity. The temperature dependence of the A_g spectra provides no evidence for anomalies associated with magnetic and/or ferroelectric ordering [18]. As reported in the literature [2], the T dependence of the most pronounced low-frequency mode at 215 cm^{-1} for $DyMn_2O_4$ could be observed. The existence of two characteristic temperatures, $T^* = -65$ K and $T_C = 39$ K showed a steep hardening upon cooling between T^* and T_C, and a softening below T_C. The latter phenomenon may be a consequence of the Mn ionic displacements and/or lattice anomalies that occur at the ferroelectric transition temperature (T_C), associated with the loss of inversion symmetry in the lattice.

PLE spectrum of $DyMn_2O_5$ nanorods was exhibited in Fig. 3(c). Excitation spectrum was wide bands located around 280–340 nm. We speculated that the excitation band might be assigned to the transition from the valence band to the conduction band for $DyMn_2O_5$ host crystal. PL spectra located at 300–400 nm could be ascribed to near band edge (NBE) emission (Fig. 3(c)). As reported in the literatures [19,20], the UV emission band corresponds to a

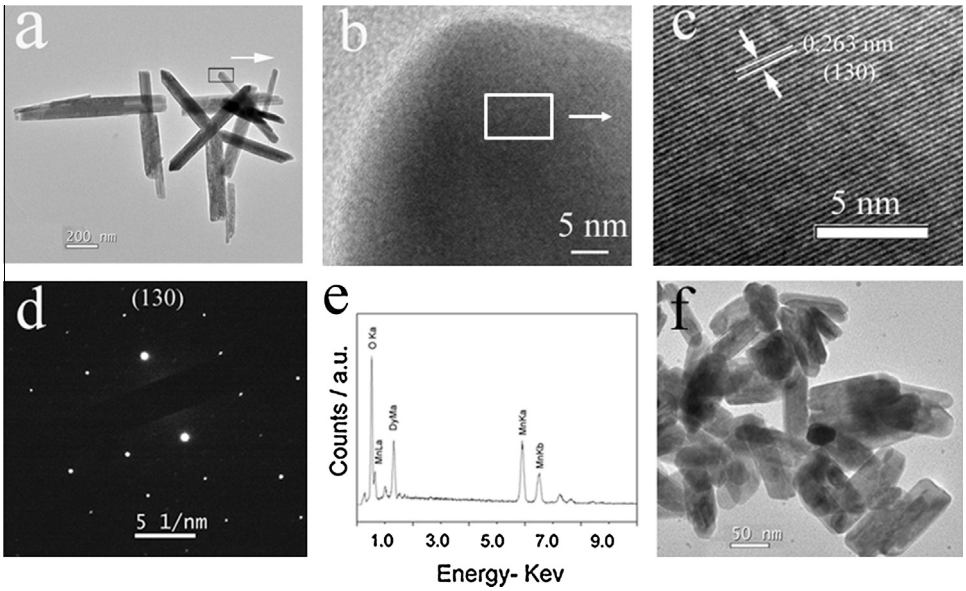

Fig. 2. (a) TEM, (b) HRTEM, (c) enlarged HRTEM images, (d) corresponding SAED pattern, (e) EDS pattern of $DyMn_2O_5$ nanorods synthesized at 250 °C for 64 h (pH = 3) and (f) TEM image of $DyMn_2O_5$ nanorods synthesized at 250 °C for 64 h (pH = 7).